Science Advances

AAAS

advances.sciencemag.org/cgi/content/full/2/7/e1600427/DC1

Supplementary Materials for

Stability of Fe,Al-bearing bridgmanite in the lower mantle and synthesis of pure Fe-bridgmanite

Leyla Ismailova, Elena Bykova, Maxim Bykov, Valerio Cerantola, Catherine McCammon, Tiziana Boffa Ballaran, Andrei Bobrov, Ryosuke Sinmyo, Natalia Dubrovinskaia, Konstantin Glazyrin, Hanns-Peter Liermann, Ilya Kupenko, Michael Hanfland, Clemens Prescher, Vitali Prakapenka, Volodymyr Svitlyk, Leonid Dubrovinsky

Published 15 July 2016, *Sci. Adv.* **2**, e1600427 (2016)
DOI: 10.1126/sciadv.1600427

This PDF file includes:

- table S2. Crystallographic data for $(Fe^{2+}_{0.64(2)}Fe^{3+}_{0.24(2)})Si_{1.00(3)}O_3$ bridgmanite at selected pressures.
- table S3. Compressibility of bridgmanite with different compositions.
- table S4. Crystallographic data of Fe_4O_5.

Supplementary Materials

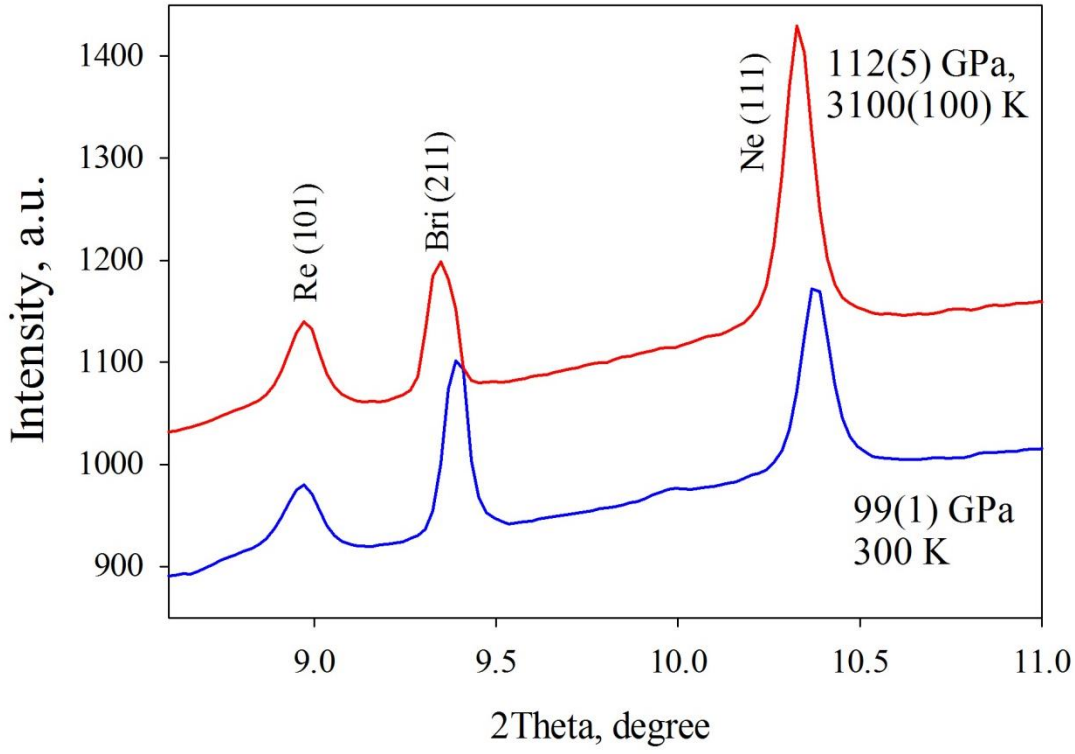

fig. S1. Parts of the integrated diffraction images of bridgmanite $Mg_{0.86}Fe_{0.14}Al_{0.04}Si_{0.96}O_3$ (FE14) collected before (lower curve) and during (upper curve) laser heating. While the position of the Re (gasket) diffraction line is not affected by heating, diffraction lines of bridgmanite and Ne (pressure transmitting and thermal insulating medium) show pronounced shifts; upon heating pressure increases from 99(1) to 112(5) GPa. Data collected at IDD-13 (APS, USA), X-ray wavelength 0.31 Å.

fig. S2 (A)

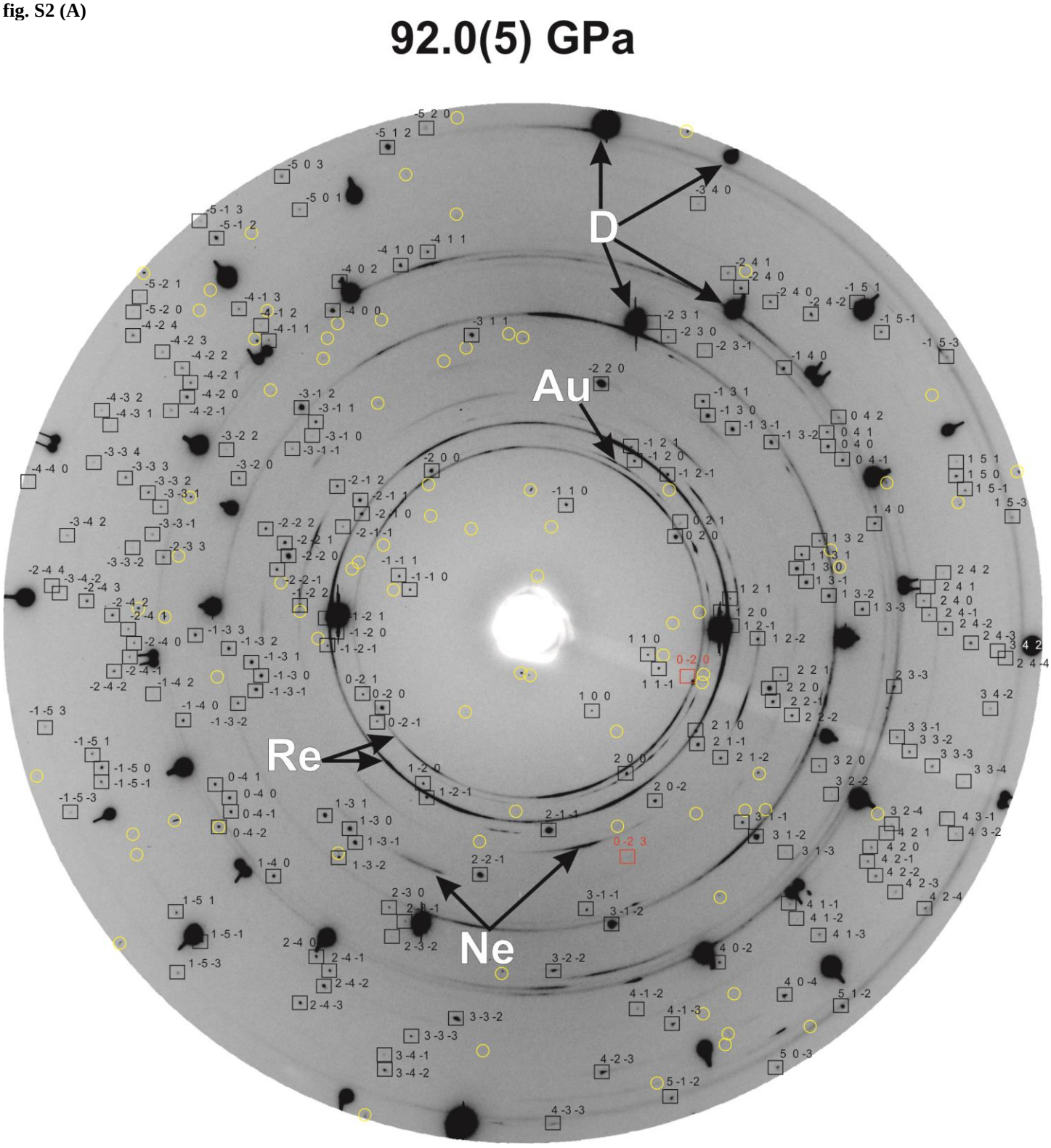

fig. S2 (B)

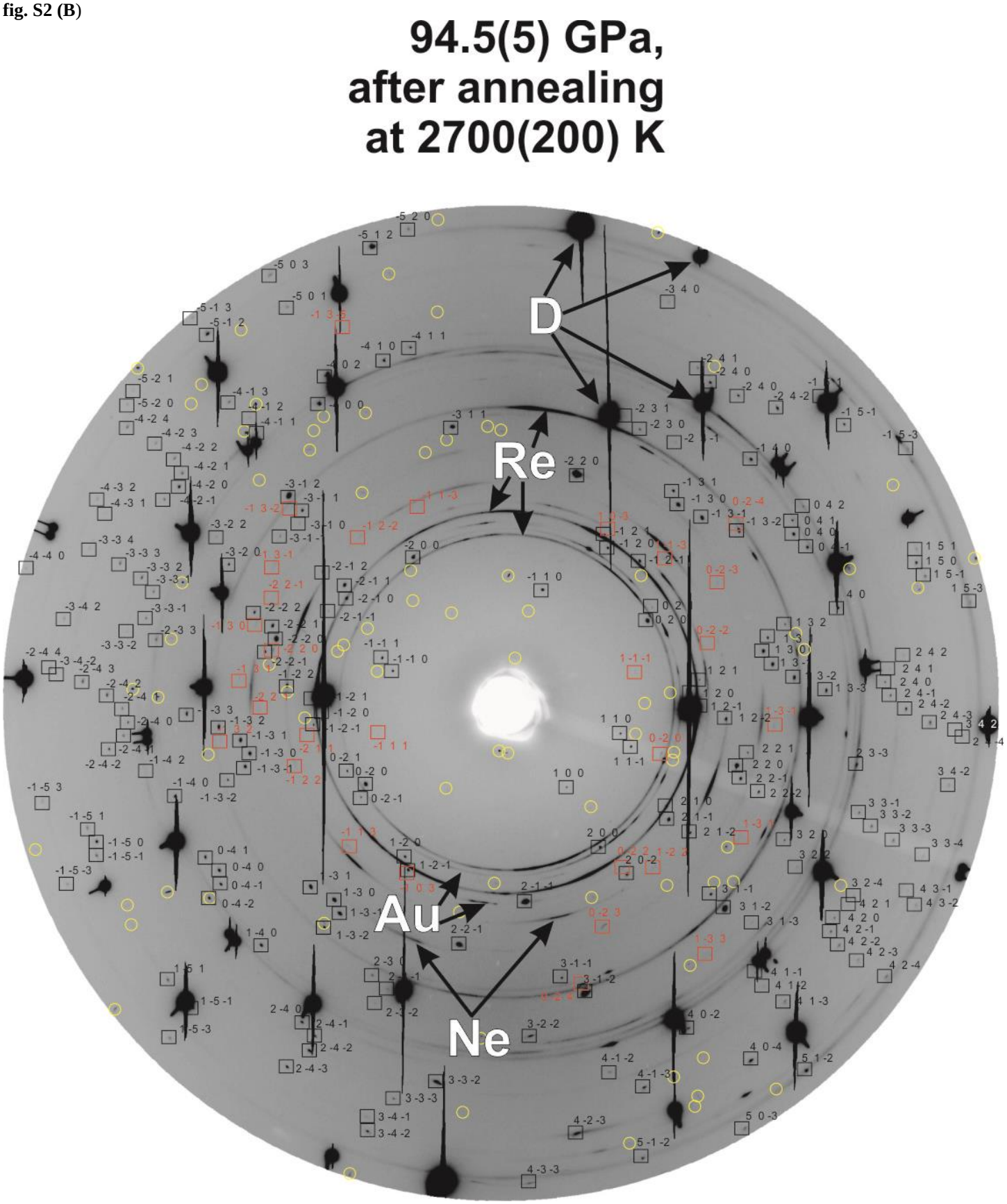

fig. S2 (C)

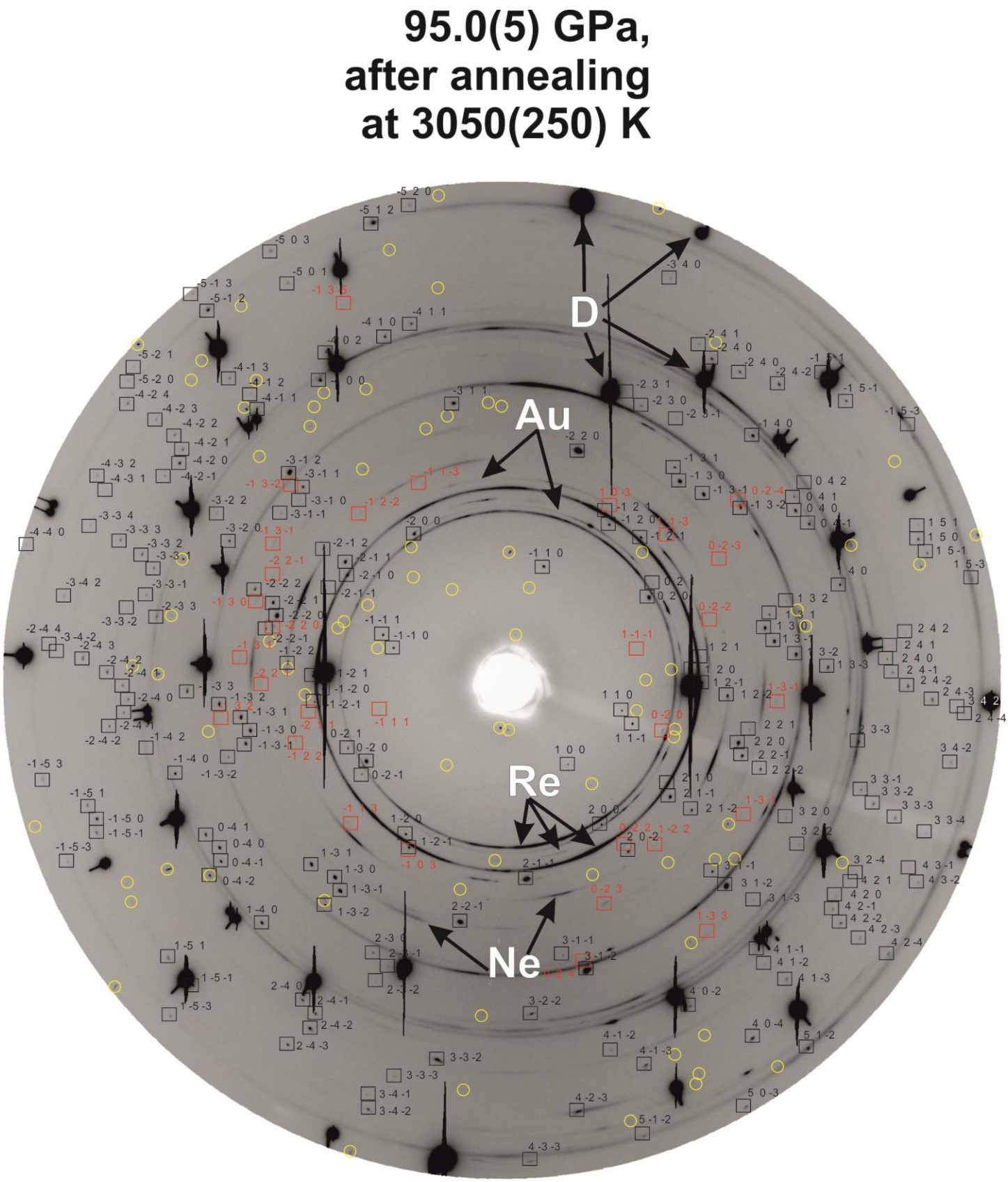

fig. S2 (D)

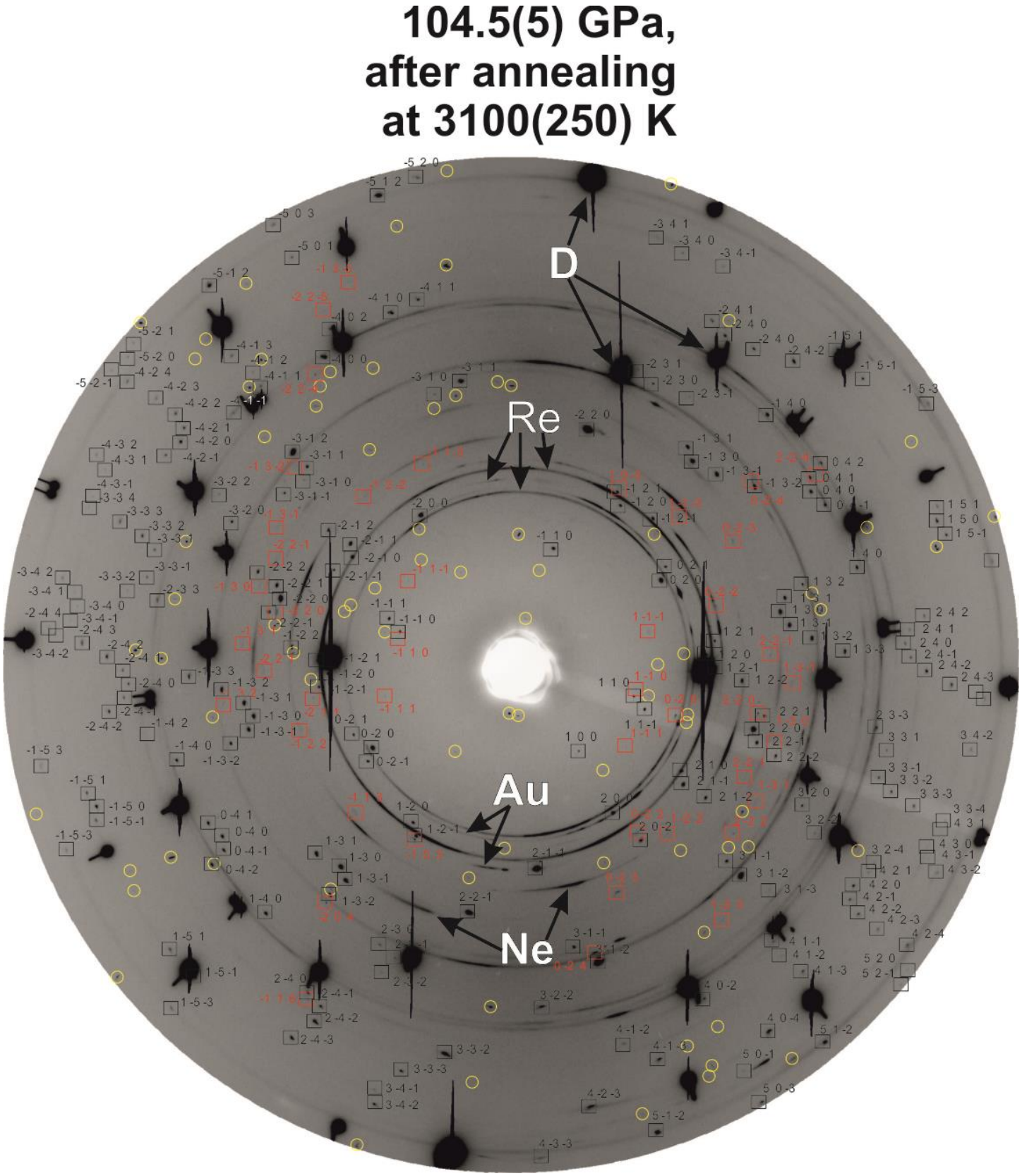

fig.S2 (E)

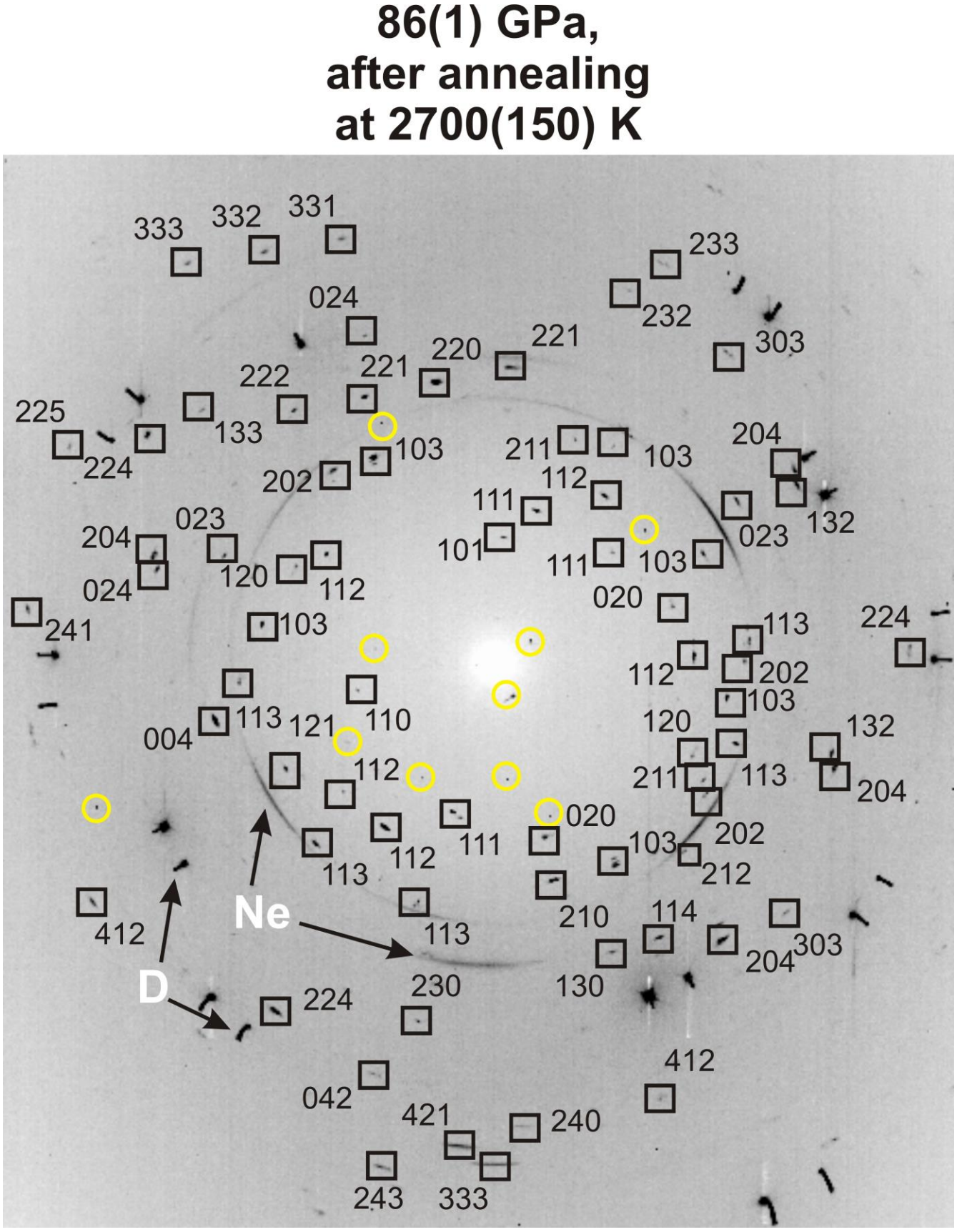
86(1) GPa,
after annealing
at 2700(150) K
333
332
331
024
233
232
303
220
221
221
222
225
133
224
103
211
103
204
202
112
111
023
132
204
023
101
111
103
120
112
024
020
241
103
113
224
112
202
103
004
113
121
110
120
132
112
211
113
204
020
202
103
111
112
212
113
210
114
Ne
303
204
412
D
230
130
224
412
042
421
240
243
333

fig.S2 (F)

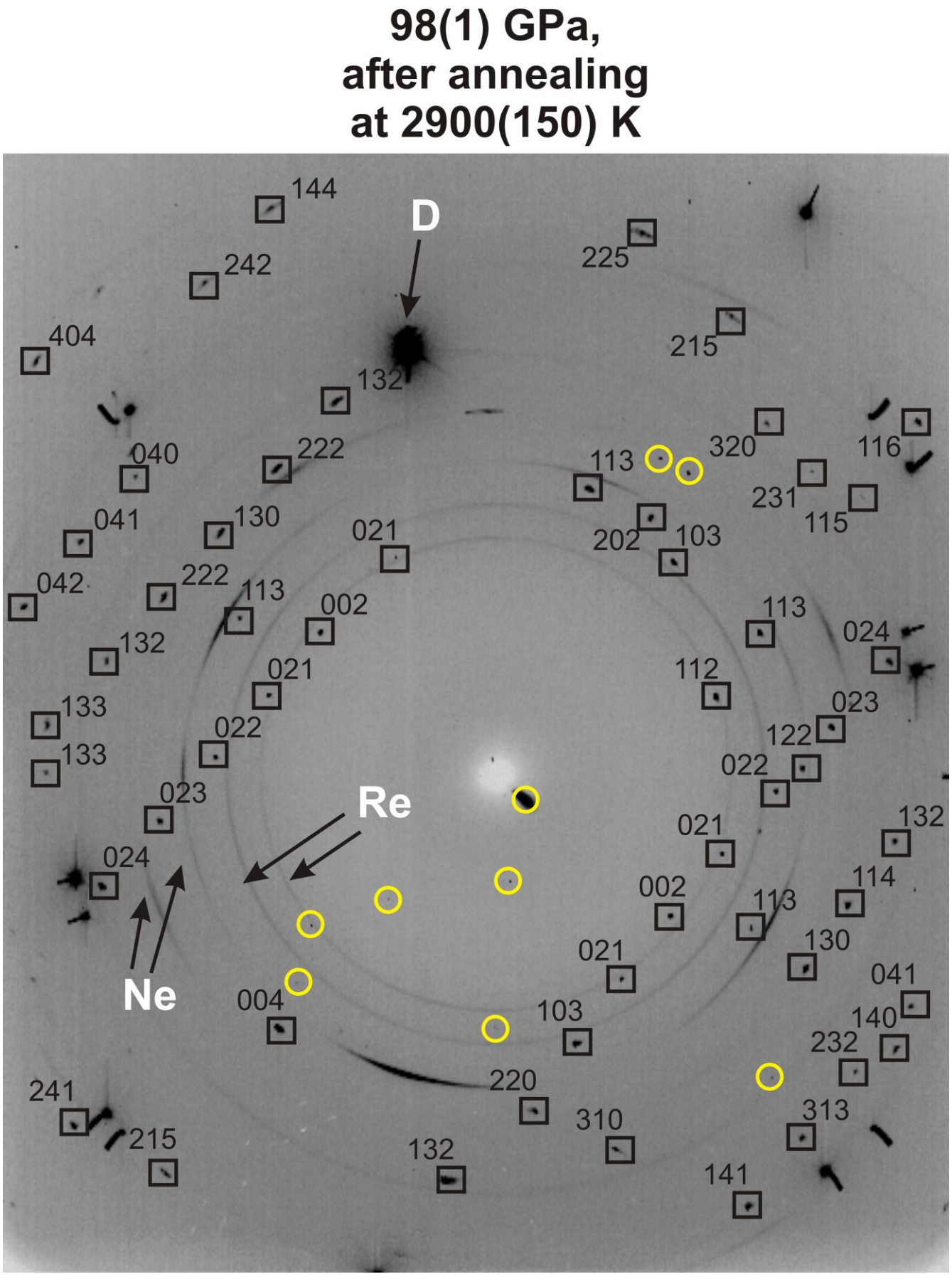
98(1) GPa,
after annealing
at 2900(150) K
D
Re
Ne
144
242
404
132
040
222
041
130
042
222
113
002
132
021
133
022
133
023
024
004
241
215
132
220
310
141
225
215
320
116
113
231
115
202
103
021
113
024
112
023
122
022
021
132
002
114
113
130
021
041
103
140
232
313

fig. S2. Full high-resolution two-dimensional wide-scan x-ray diffraction images of bridgmanite samples FE14, FE17, and FE40. Data were collected (**A**) before and (**B**-**D**) after laser heating for sample FE14, and for samples FE17 (**E**) and FE40 (**F**) after laser heating at the indicated temperatures and pressures. Indices are given for bridgmanite reflections (underlined by boxes). The only observed changes in diffraction patterns upon heating are due to development of additional domains of the same phase (marked in red). Large black spots are due to diamond reflections. Diffraction rings of Ne (pressure transmitting medium), Re (gasket), and Au are also marked. Data were collected at IDD-13 at APS (A-D) and ID09 at ESRF (E,F). Yellow circles indicate bad pixels of the detector.

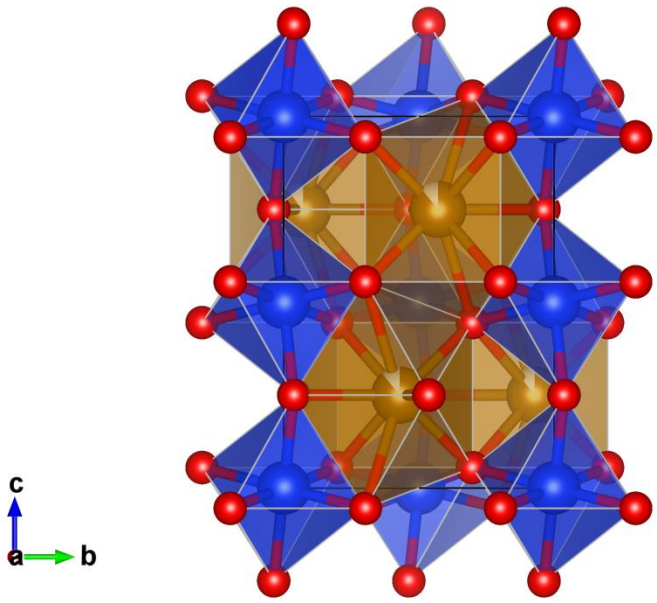

fig. S3. Representative polyhedral structural model of orthorhombic bridgmanite. The bridgmanite structure (space group *Pbmn*, #62) has two cation positions – a distorted bi-caped prism ("A"-site, brown) and octahedra ("B-site", blue). Red balls represent oxygen atoms. For the case of $(Fe^{2+}_{0.64(2)}Fe^{3+}_{0.24(2)})Si_{1.00(3)}O_3$ bridgmanite (synthesized, for example, at 67 GPa and 2200(100)K; orthorhombic *Pbnm*, *a=4.5516(3)* Å, *b=4.7753(15)* Å, *c=6.5497(4)* Å, *V=142.36(5)* $Å^3$) vacancies on the A-site are indicated in white.

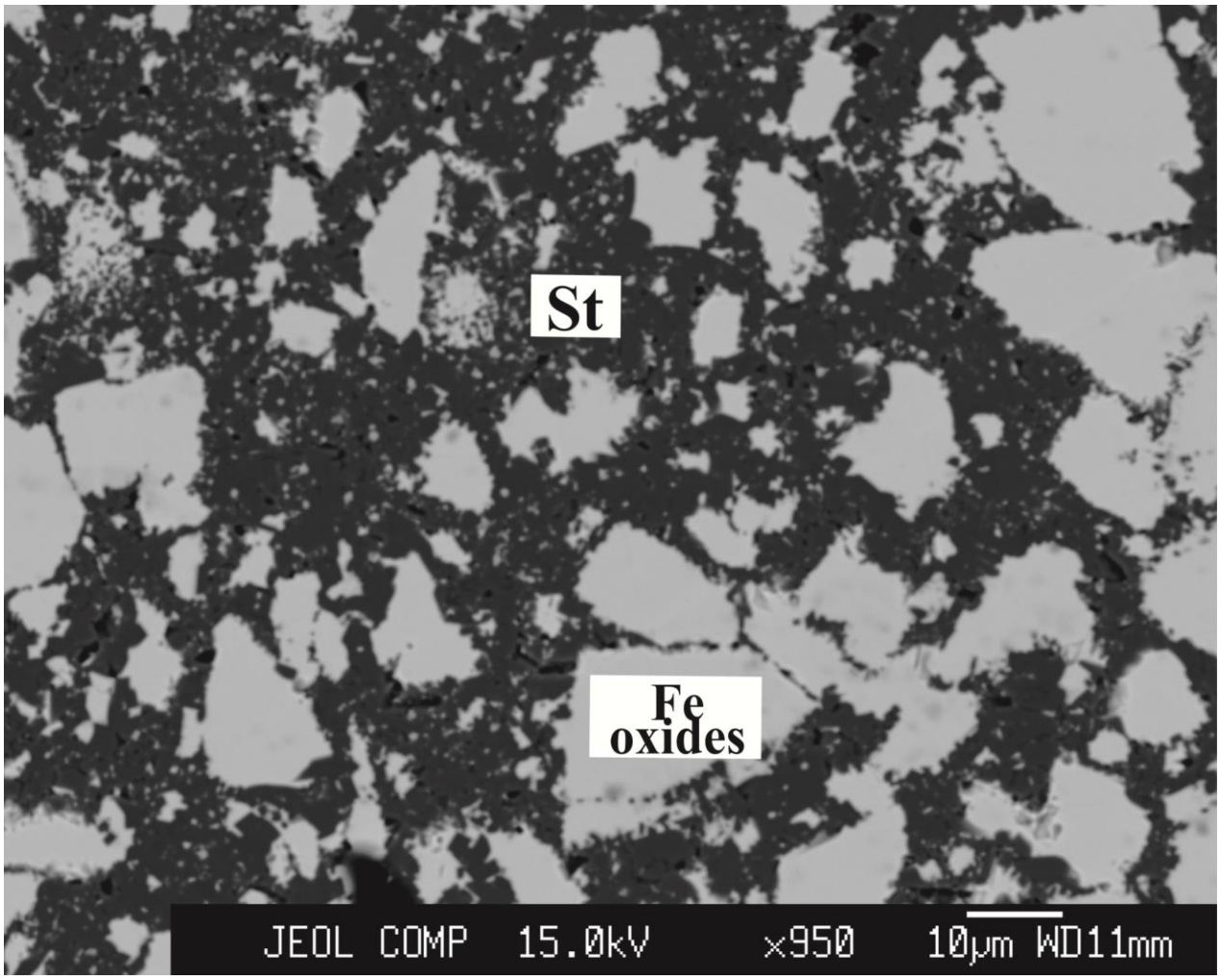

fig S4. Backscattered electron image of skiagite starting composition at 23 GPa and 1600°C (run S6151). Skiagite-majorite garnet decomposes to oxides: dark gray – SiO_2 (stishovite), light gray – Fe oxides ($Fe_{1-x}O$ and Fe_4O_5).

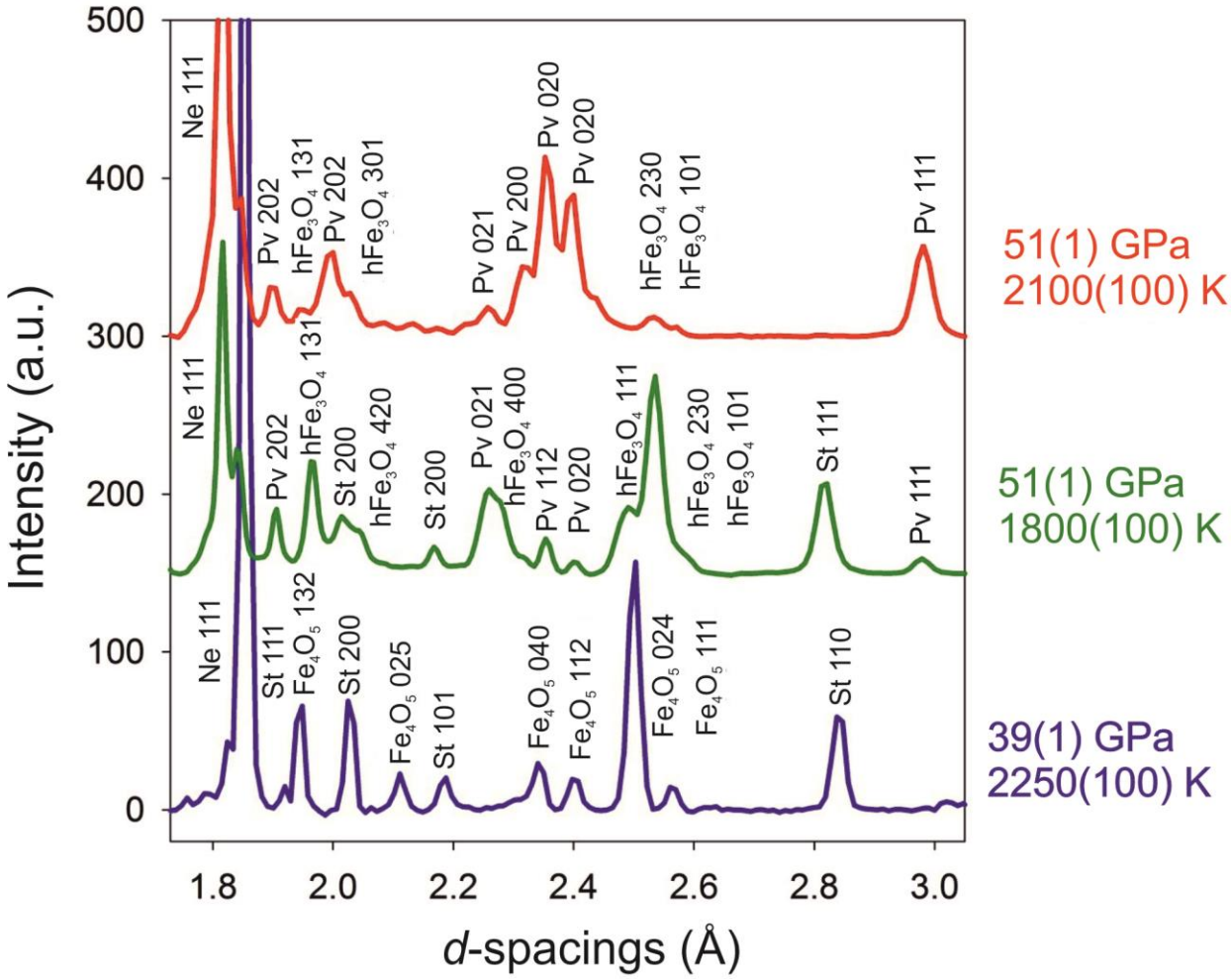

fig. S5. Typical powder x-ray diffraction patterns of skiagite-majorite garnet that was laser-heated at different pressures and temperatures (St, stishovite; hFe_3O_4, orthorhombic $CaTi_2O_4$-type Fe_3O_4, Pv, perovskite-structured phase). Pressure was determined using Ne lattice parameters (see http://kantor.50webs.com/diffraction.htm).

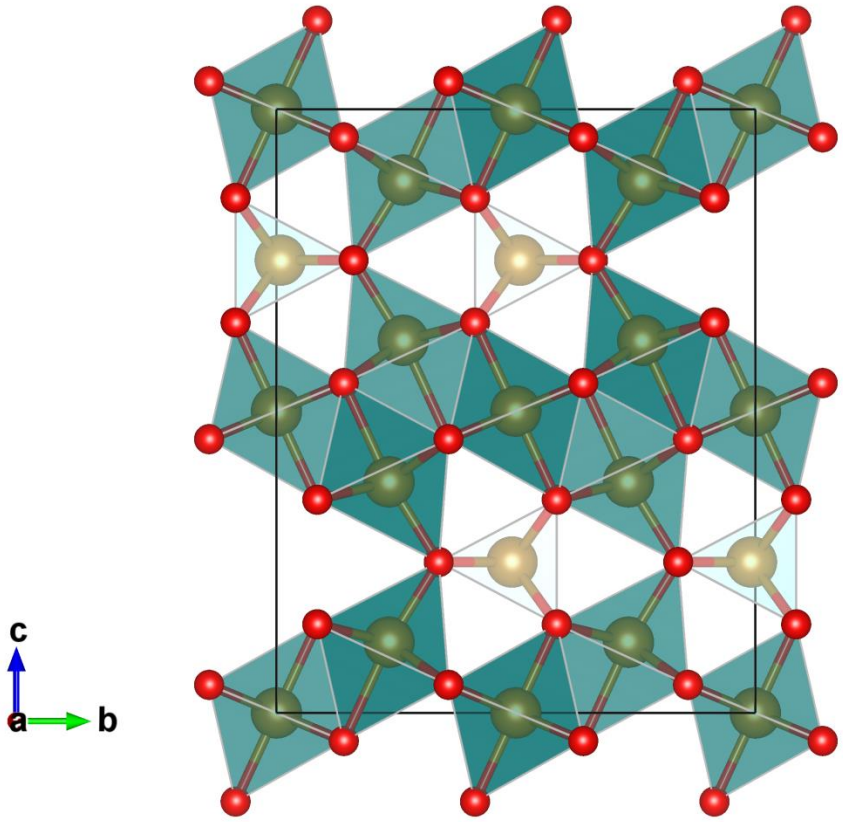

fig S6. Crystal structure of Fe_4O_5 obtained as the product of decomposition of skiagite-majorite garnet in a laser-heated DAC at 39(1) GPa and 2250(100) K (see table S4 for crystallographic data). Fe1 occupy trigonal-prismatic sites (light green) and Fe2 and Fe3 occupy the two slightly different octahedral sites (green). Red balls represent oxygen atoms.

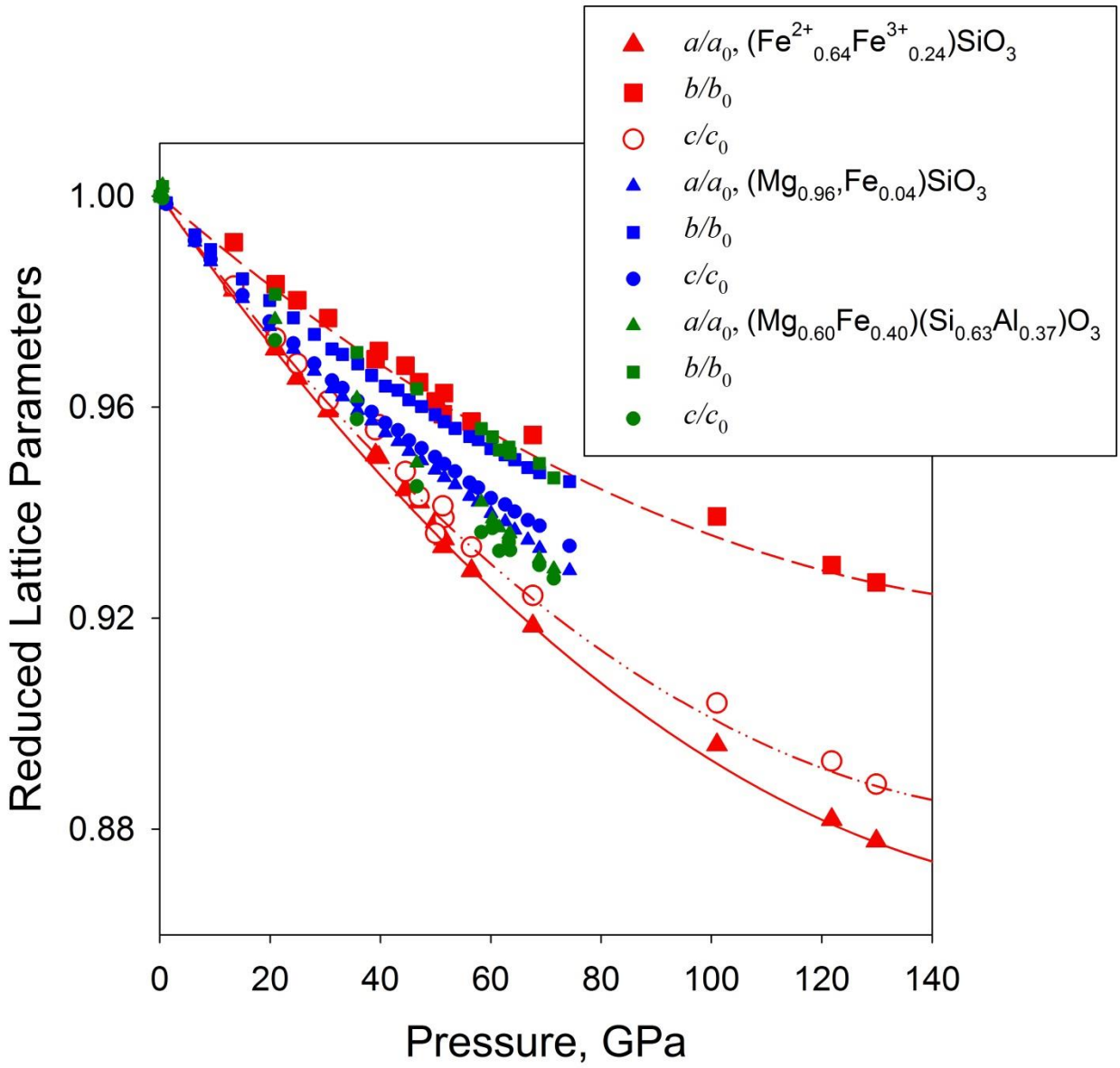

fig.S7. Variation with pressure of the normalized unit-cell parameters for three bridgmanites—Fe-bridgmanite (this study), $(Mg_{0.96},Fe_{0.04})SiO_3$ (*32*), and $Mg_{0.60}Fe_{0.40}Si_{0.63}Al_{0.37}O$. (*12*) Note the clearly different behavior of the *a*- and *b*-axis of Fe-bridgmanite.

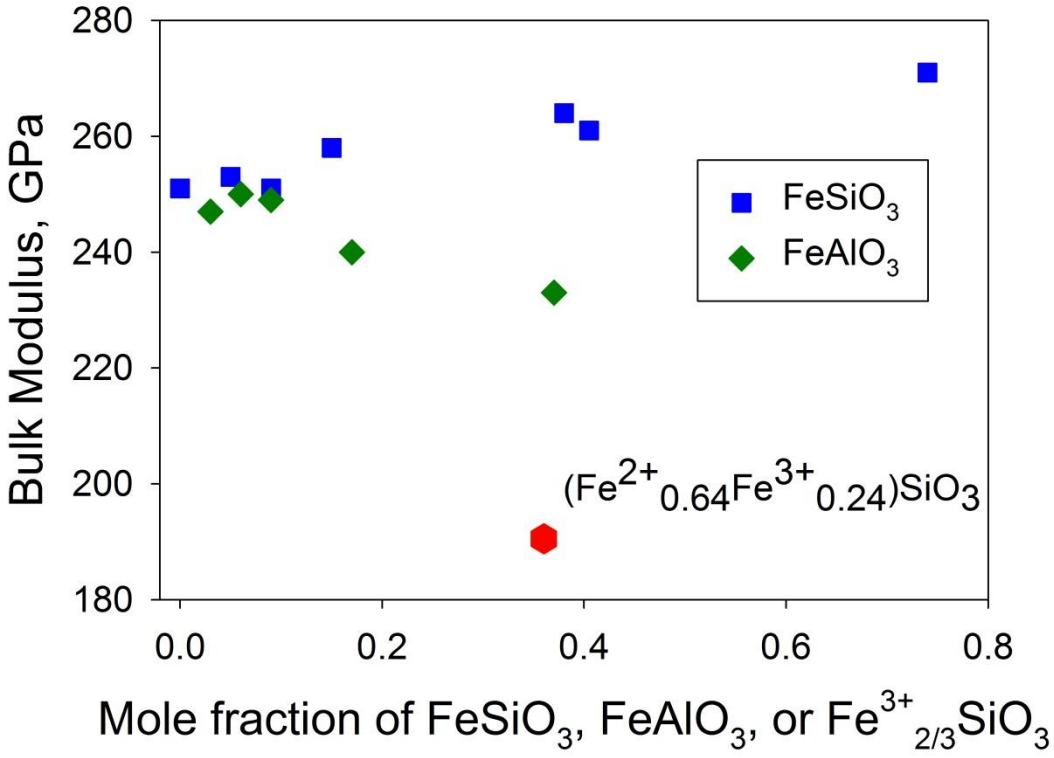

fig. S8. Effect of $Fe^{A}SiO_3$, $Fe^{A}Al^{B}O_3$, and $Fe^{3+,A}_{2/3}SiO_3$ substitutions in bridgmanite on the bulk modulus ("A" and "B" denote structural positions; see table S3 for references).

Supplementary Tables

table S1. Crystallographic data for Fe,Al bridgmanite samples FE14, FE17, and FE40 at selected pressures before and after laser heating at different temperatures.

Crystallographic data	FE14	FE14	FE14	FE14	FE40	FE17	FE17
P, T conditions of data acquisition	92.0(5) GPa	94.5(5) GPa, after 30 min heating at 2700(200) K	95.0(5) GPa after 40 min heating at 3050(250) K	104.5(5) GPa, after 30 min heating at 3100(250) K	101(2) GPa after 30 min heating at 2800(150) K	109(1) GPa	108(2) GPa after 40 min heating at 2600(100) K
Crystal system	Orthorhombic						
Space group	*Pbnm*						
a (Å)	4.3955(7)	4.3944(7)	4.3931(6)	4.3615(5)	4.385(7)	4.3446(10)	4.3476(7)
b (Å)	4.6336(6)	4.6313(6)	4.6313(6)	4.6103(5)	4.6758(12)	4.617(2)	4.6014(8)
c (Å)	6.397(4)	6.390(5)	6.395(5)	6.359(4)	6.378(2)	6.3405(16)	6.3398(7)
V (Å^3)	130.28(9)	130.04(11)	130.11(9)	127.86(8)	130.8(2)	127.18(7)	126.83(3)
Z	4						
Fe occupancy in A position, %	14.4±1.1	14.4±1.1	13.4±1.1	13.7±1.1	38±1.2	17±2	17.1±1.2
Atomic coordinates(xyz)	Mg/Fe 0.5212(3) 0.5722(3) 0.25	Mg/Fe 0.5207(3) 0.5721(3) 0.25	Mg/Fe 0.5208(3) 0.5718(4) 0.25	Mg/Fe 0.5215(3) 0.5731(4) 0.25	Mg/Fe -0.011(2) 0.4237(8) 0.25	Mg/Fe -0.0219(9) 0.4278(12) 0.25	Mg/Fe -0.0218(4) 0.4247(6) 0.25
Mg/Fe	Si/Al 0.5	Si/Al 0.5	Si/Al 0.5	Si/Al 0.5	Si/Al 0	Si/Al 0	Si/Al 0
Si/Al							
O1	0 0.5	0 0.5	0 0.5	0 0.5	0 0	0 0	0 0
O2	O1 0.1148(8) 0.4661(7) 0.25 O2 0.1852(6) 0.1936(5) 0.5571(8)	O1 0.1139(8) 0.4660(6) 0.25 O2 0.1846(5) 0.1938(4) 0.5567(8)	O1 0.1145(9) 0.4667(7) 0.25 O2 0.1844(6) 0.1933(5) 0.5572(9)	O1 0.1155(8) 0.4665(7) 0.25 O2 0.1837(6) 0.1931(5) 0.5574(8)	O1 0.125(7) 0.052(3) 0.25 O2 0.188(4) 0.311(2) -0.0585(12)	O1 0.111(3) 0.037(3) 0.25 O2 0.1829(14) 0.305(2) -0.0569(11)	O1 0.1163(9) 0.0320(11) 0.25 O2 0.1832(6) 0.3072(6) -0.0571(4)
F(000)	208	208	207	207	220	211	211
Theta range for data collection (°)	2.78 11.261	2.787 11.232	2.784 10.949	2.804 11.285	3.73 18.57	3.32 19.11	0.454 19.05
Completeness to *d* = 0.8 Å, %	61.9	61.1	61.8	61.1	31.8	40.6	45.4

Crystallographic data	FE14	FE14	FE14	FE14	FE40	FE17	FE17
Index ranges	-5< *h* < 5, -5< *k* < 5, -4 < *l* < 4	-5< *h* < 5, -5< *k* < 5, -4 < *l* < 4	-5 < *h* < 5, -5 < *k* < 5, -4 < *l* < 4	-5 < *h* < 5, -5 < *k* < 5, -4 < *l* < 4	-2< *h* < 3, -6< *k* < 6, -8< *l* < 7	-5< *h* < 6, -4< *k* < 5, -7< *l* < 8	-5< *h* < 5, -5< *k* < 4, -7< *l* < 8
No. of measured, independent, and observed [I >2σ(I)] reflections	252/91/82	242/88/81	245/89/82	243/88/83	176/104/94	207/113/90	221/124/124
R_{int}	0.0367	0.0307	0.0334	0.0331	0.0685	0.0510	0.0621
No.of parameters/restraints	0/13	0/13	0/13	0/13	0/12	0/13	0/14
Goodness of fit on F^2	1.319	1.194	1.143	1.144	0.959	1.021	1.184
Final *R* indices [$I > 2\sigma(I)$] R_1 / wR_2	0.0373/ 0.0979	0.0415/ 0.1067	0.0443/ 0.1076	0.0415/ 0.1043	0.0638/ 0.1396	0.1055/ 0.0975	0.0629/ 0.1731
R indices (all data) R_1 / wR_2	0.0563 / 0.1183	0.0471 / 0.1100	0.0506 / 0.1117	0.0428/ 0.1056	0.0730/ 0.1632	0.2420/ 0.2295	0.0629/ 0.1731
Largest diff. peak /hole (e / Å^3)	0.998 / -0.778	0.600/ -0.504	0.594/ -0.672	0.603/ -0.590	0.442/ -0.648	1.707/ -1.057	0.884/ -0.961

table S2. Crystallographic data for $(Fe^{2+}_{0.64(2)}Fe^{3+}_{0.24(2)})Si_{1.00(3)}O_3$ bridgmanite at selected pressures**.**

P, T conditions of XRD experiment	44.0(5) GPa	67.0(5) GPa 2200(100) K	107.0(5) GPa 2300(100) K	129.0(5) GPa 1835(100) K
Crystal system		Orthorhombic		
Space group		*Pbnm*		
a (Å)	4.6332(17)	4.5516(3)	4.4364(6)	4.3494(15)
b (Å)	4.815(5)	4.7753(15)	4.7079(10)	4.6354(14)
c (Å)	6.654(3)	6.5497(4)	6.328(5)	6.296(6)
V (Å^3)	148.44(18)	142.36(5)	132.17(11)	126.93(13)
Z		4		
Fe occupancy in A position, %	85.3±1.7	88.7±1.4	84.3±1.1	82.1±1.3
Atomic coordinates(xyz) Fe Si O1 O2	Fe -0.0147(4) 0.4366(8) 0.25 Si 0 0 0 O1 0.110(2) 0.041(3) 0.25 O2 0.1861(14) 0.314(2) -0.0537(10)	Fe -0.0196(3) 0.4295(8) 0.25 Si 0 0 0 O1 0.1125(15) 0.038(3) 0.25 O2 0.1853(8) 0.302(2) -0.0546(5)	Fe -0.0250(4) 0.4224(4) 0.25 Si 0 0 0 O1 0.1198(18) 0.0356(16) 0.25 O2 0.1813(13) 0.3090(10) -0.0559(15)	Fe -0.0280(5) 0.4182(5) 0.25 Si 0 0 0 O1 0.123(2) 0.0375(15) 0.25 O2 0.1797(18) 0.3089(11) -0.0567(19)
A-bicapped prism, V_0, Å^3	15.7297	15.258	14.0290	13.4375
B-octahedra, V_0, Å^3	7.2301	6.888	6.5024	6.2801
F(000)	268	268	268	268
Theta range for data collection (°)	to 3.127 to 15.005	3.181 to 20.238	3.683 to 20.152	3.749 to 15.185
Completeness to *d* = 0.8 Å, %	68.5	52.5	66.2	65.1
Index ranges	-5 < *h* < 5, -4 < *k* < 4, -6< *l* < 7	-7< *h* < 6, -4 < *k* < 3, -10 < *l* < 10	-6 < *h* < 7, -7< *k* < 7, -4 < *l* < 4	-4 < *h* < 5, -5 < *k* < 5, -4 < *l* < 5
No. of measured, independent,	265/110/99	349/138/130	310/137/126	208/93/90

and observed [I > 2σ(I)] reflections				
R_{int}	0.0274	0.0437	0.0352	0.0464
No.of parameters/restraints	14 / 0	15 / 0	13 / 0	14 / 0
Goodness of fit on F^2	1.119	1.162	1.205	1.144
Final R indices [$I > 2\sigma(I)$] R_1 / wR_2	0.0828 / 0.1936	0.0735 / 0.1912	0.0618 / 0.1705	0.071 /0.1792
R indices (all data) R_1 / wR_2	0.0882 / 0.1981	0.0746 / 0.1923	0.0661 / 0.1748	0.0726 / 0.1821
Largest diff. peak /hole (e / Å^3)	1.274 / -0.857	1.480 / -1.265	0.923 / -1.510	1.043 / -0.994

table S3. Compressibility of bridgmanite with different compositions.*

Composition	Bulk		A-bicapped prism		B-octahedra		Reference
	K_{300}, GPa	V_0, Å^3/unit cell	K_{300}, GPa	V_0, Å3	K_{300}, GPa	$V_{0,}$ Å3	
$(Fe^{2+}_{0.64(2)}Fe^{3+}_{0.24(2)})SiO_3$	190(4)	178.98(6)	178(5)	19.25(5)	230(9)	8.51(5)	This work
$(Mg_{0.86}Fe_{0.14})(Si_{0.96}Al_{0.04})O_3$	250(4)	164.49(5)	219(6)	17.92(9)	335(8)	7.69(2)	This work
$(Mg_{0.60}Fe_{0.40})(Si_{0.63}Al_{0.37})O_3$	233	169.9	217(5)	18.13(5)	285(12)	8.23(4)	(*12*, *36*)
$MgSiO_3$	251	162.36	262(5)	17.57(11)	327(5)	7.67(3)	(*32*, *47*)
$(Mg_{0.96},Fe_{0.04})SiO_3$	253	163.09					(*32*)
$(Mg_{0.85},Fe_{0.15})SiO_3$	258	163.3					(*10*)
$(Mg_{0.91},Fe_{0.09})SiO_3$	251	163.0					(*21*)
$(Mg_{0.62},Fe_{0.38})SiO_3$	264	164.7					(*21*)
$(Mg_{0.26},Fe_{0.74})SiO_3$	271	166.7					(*21*)
$(Mg_{0.95}Fe_{0.07})(Si_{0.93}Al_{0.05})O_{2.97}$	247	163.68					(*33*)
$(Mg_{0.87}Fe_{0.13})(Si_{0.89}Al_{0.11})O_3$	249	164.55					(*33*)
$(Mg_{0.77}Fe_{0.24})(Si_{0.82}Al_{0.17})O_3$	240	168.84					(*33*)
$(Mg_{0.75}Al_{0.25})(Si_{0.75}Al_{0.25})O_3$	253	164.85					(*10*)
$(Mg_{0.345}Fe_{0.405}Al_{0.25})(Si_{0.75}Al_{0.25})O_3$	261	165.6					(*10*)
$(Fe_{0.75}Al_{0.25})(Si_{0.75}Al_{0.25})O_3$	252	170.5					(*10*)

* Data fitted with Birch-Murnaghan equation of state with fixed K'=4.

table S4. Crystallographic data of Fe_4O_5.

Empirical formula	Fe_4O_5
P, T conditions of XRD experiment	39 GPa 2250(100) K
Crystal system	orthorhombic
Space group	*Cmcm*
a (Å)	2.7379(6)
b (Å)	9.4010(19)
c (Å)	11.846(4)
V (Å^3)	304.90(13)
Z	4
Fractional atomic coordinates (*x y z*):	
Fe1	1 0.5 0.5
Fe2	0 0.0080(3) 0.75
Fe3	0.5 0.2649(3) 0.6172(2)
O4	0.5 0.1610(19) 0.75
O5	0.5 0.3594(11) 0.4535(12)
O6	1 0.4147(12) 0.6468(11)
F(000)	576
Theta range for data collection (°)	4.528 to 20.916
Completeness to *d* = 0.8 Å, %	47.1
Index ranges:	-3 < *h* < 3,
	-14 < *k* < 10,
	-13< *l* <17
No. of measured, independent, and observed [I > 2σ(I)] reflections	425/231/173
No. of parameters/restraints	32/0
R_{int}	0.0578
Goodness of fit on F^2	1.126
Final *R* indices [$I > 2\sigma(I)$] R_1 / wR_2	0.0874/0.2430
R indices (all data) R_1 / wR_2	0.1007/0.2571